# Observation of anomalous reactivities of Ni/Pt(111) bimetallic surfaces

B. Frühberger *, J. Eng Jr. and J.G. Chen ‡

*Corporate Research Laboratories, Exxon Research and Engineering Company, Annandale, NJ 08801, USA*
E-mail: jchen@erenj.com

Received 20 November 1996; accepted 3 March 1997

We have investigated the surface reactivities of Ni/Pt(111) bimetallic model catalysts using ethylene and cyclohexene as probing molecules. The bimetallic surfaces were generated by evaporating Ni onto a Pt(111) single-crystal surface held at 600 K. The surface chemistry was investigated using high-resolution electron energy loss spectroscopy (HREELS), Auger electron spectroscopy (AES), temperature-programmed desorption (TPD) and low-energy electron diffraction (LEED). The reactivities of the bimetallic surfaces were compared with those of the clean Pt(111) surface and a thick Ni(111) film on the Pt(111) substrate. Formation of the bimetallic surface led to a significantly reduced reactivity towards the decomposition of ethylene when compared to either Pt(111) or Ni(111)/Pt(111) surfaces. Furthermore, although the surface reactivity towards cyclohexene was retained for the bimetallic surface, the decomposition mechanism was distinctly altered from that of either Pt(111) or Ni(111)/Pt(111) surfaces.

**Keywords:** Ni/Pt(111), surface reactivities, ethylene, cyclohexene, HREELS, AES, TPD, LEED

## 1. Introduction

The study of the chemical properties of bimetallic surfaces has drawn considerable attention, particularly since the development of bimetallic catalysts for hydrocarbon reforming in the 1970's [1–4]. Catalytic properties of bimetallic systems have been found to differ strongly from either pure metal component in some cases. In recent years, increasing numbers of surface science studies have been published [5–7], driven by the desire to gain a more fundamental understanding of the structural, electronic and chemical properties of bimetallic surfaces. The preparation, characterization and reactivities of bimetallic surfaces have been recently reviewed by Rodriguez [7].

Motivated by these studies, we have investigated the surface reactivity of Ni/Pt bimetallic surfaces produced by thermal evaporation of Ni onto a Pt(111) substrate. Generation of model bimetallic surfaces in such a manner offers several advantages over the use of bulk alloy systems. For example, it frequently enables one to prepare and study bimetallic surfaces that have no stable bulk analogue [7]. In addition, it allows one to readily compare the reactivities with those of either pure metal components, and to investigate surface chemistry as a function of different bimetallic atomic ratios. In the current study, we investigated the surface reactivity of Ni/Pt(111) bimetallic surfaces by using ethylene and cyclohexene as chemical probes. As we will show in this paper, the Ni/Pt(111) bimetallic surface is characterized by a unique surface chemistry that is distinct from either Pt(111) or Ni(111) surfaces.

## 2. Experimental

Experiments were carried out in an ultra-high vacuum (UHV) system with a base pressure of $\leqslant 2 \times 10^{-10}$ Torr, as described previously [8]. Briefly, the chamber contains an LK 3000 HREELS spectrometer for vibrational analysis, a double-pass cylindrical mirror analyzer (CMA, Physical Electronics) for Auger and photoemission measurements, low-energy electron diffraction (LEED) optics and a random flux shielded quadrupole mass spectrometer (QMS). Primary beam energy for all AES measurements was 5 kV. HREELS spectra were collected in the specular direction with an incident angle of 60° and a primary beam energy of 6 eV. Spectral resolution was typically 24–32 $cm^{-1}$. For TPD experiments, the random flux shield of the residual gas analyzer was kept at a distance of $\sim$ 5 mm from the sample surface. A linear heating rate of 3 K/s was used throughout. Our experimental set-up allowed to monitor up to 16 masses simultaneously.

The single-crystal Pt sample was oriented along the (111) direction, 1.5 mm thick platinum disk (99.999%), 12 mm in diameter. It could be heated resistively and cooled with liquid $N_2$. Sample temperature was measured with a type K thermocouple spot-welded to the back of the crystal. The surface was cleaned by repeated cycles of $Ne^+$ ion sputtering at 1000 K (3 kV, $\sim$ 6 mA) and annealing at 1250 K. Remaining trace amounts of

* Current address: The BOC Group Technical Center, 100 Mountain Avenue, Murray Hill, NJ 07974, USA.
‡ To whom correspondence should be addressed.

carbon were removed by exposure to oxygen at 1000 K and subsequent heating to 1200 K. Sample cleanliness was verified by AES and HREELS. All gases used were of research grade purity and were introduced into the UHV chambers without further purification. Cyclohexene (ALDRICH, 99.99%) was purified by several freeze–pump–thaw cycles. Purity was checked by in situ mass spectrometry. Exposures given are from uncorrected ion gauge readings.

Nickel was deposited from an evaporative doser which consisted of a resistively heated tungsten filament, tightly wrapped with ultra-pure Ni wire (99.999% Ni), mounted in a stainless steel enclosure with an opening of 1 cm in diameter. After initial thermal conditioning, the amount of impurity buildup (mainly carbon) was below or near the detection limit of AES, with the C/Ni atomic ratio always less than 0.03. During deposition, the Pt(111) crystal was positioned approximately 5 cm from the Ni doser opening, with the sample surface perpendicular to the doser axis.

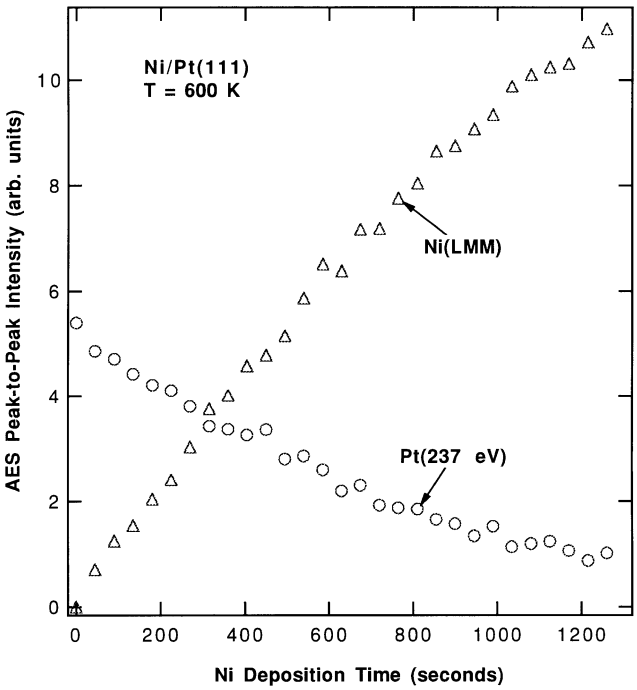


Figure 1. AES uptake curve following the deposition of Ni on Pt(111) at 600 K.

## 3. Results and discussion

### *3.1. Preparation of the Ni/Pt(111) bimetallic surfaces*

Ni/Pt(111) bimetallic surfaces were prepared by thermal evaporation of ultra-pure Ni onto the Pt(111) substrate, maintained at 600 K. The LEED pattern remained (1 × 1) for all Ni coverages obtained in this fashion. Surface order was reduced, however, as indicated by slightly less well defined LEED spots. In a recent photoelectron diffraction study [9], the growth mode for Ni deposition on Pt(111) at room temperature has been shown to be layer-by-layer (Frank-van der Merwe mode) for at least the first two monolayers. We attempted to verify this growth mode of Ni in our experiments at 600 K, by monitoring the Pt(237 eV) and Ni(LMM) Auger peak-to-peak intensities as a function of deposition time for a constant power setting of our Ni evaporator. For each consecutive dosing and AES measurement cycle, only the vertical position of the Pt(111) crystal was changed to move the crystal between the position for Ni dosing and AES measurement. The solid angle of Ni evaporation was large compared to the crystal diameter, so that errors in vertical height positioning could be assumed to be negligible. Ni deposition was uniform across the substrate surface, as verified with AES. The Ni evaporation rate for each dose was constant within the experimental error during these experiments, as verified by comparing the Pt(237 eV)/Ni(LMM) Auger peak-to-peak intensity ratios for several doses onto the clean Pt(111) substrate at constant evaporator power. The result of the obtained Auger signal–time plot is shown in figure 1. We would expect the Pt(237 eV) Auger signal intensity to be attenuated to ~ 66% of the clean surface value at completion of the first epitaxial monolayer [10], assuming an inelastic mean free path (IMFP) for the Pt(237 eV) Auger electrons of 6.2 Å [11] and an atomic radius of 1.11 Å for Ni (obtained from the specific gravity of Ni). In a layer-by-layer growth model, these mean free path values would lead to a Ni(LMM)/Pt(237 eV) Auger peak-to-peak intensity ratio of approximately 1.0 at one monolayer Ni coverage. However, as shown in figure 1, the signal–time plot following the deposition of Ni at 600 K can not readily be fitted to a layer-by-layer model or to any other typical growth model. Furthermore, we do not believe that our data allows one to conclusively exclude the possibility of layer-by-layer growth at 600 K, given the uncertainties involved in using Auger signal–time plots for growth mode determinations. Problems, such as ambiguities in assigning the breakpoints or their dependencies on the detection angle for the Auger electrons, are well documented in the literature [12]. Given the described uncertainties in growth mode, we were unable to calibrate the absolute Ni coverage on our model bimetallic surfaces. We will therefore only report Ni(LMM)/Pt(237 eV) Auger peak-to-peak intensity ratios for these surfaces.

When the sample temperature was raised above ~ 700 K, the Ni(LMM)/Pt(237 eV) Auger peak-to-peak intensity began to decrease. The rate of decrease was enhanced with increasing temperature. Ni is assumed to dissolve into the sample bulk, since no Ni desorption was observed by mass spectrometry up to temperatures of 1200 K. It is important to point out that the surface reactivities of Ni/Pt(111) were similar, as long as the surfaces were characterized by similar Ni/Pt AES ratios. They

are independent of whether the specific Ni(LMM)/Pt(237 eV) Auger peak-to-peak intensity ratio was achieved by direct dosing at 600 K, or by annealing a sample with higher Ni coverages until the specific Ni/Pt ratio was obtained. We believe this to be an indication of surface alloying at our dosing temperature of 600 K, at least at early stages of growth. Surface alloying at temperatures well below our dosing temperature of 600 K is well documented in the literature for a variety of systems [13], even for systems like Au on Ni(111) for which the heat of solution is large and positive [14].

At sufficiently high Ni coverages, a thick Ni(111) film can be produced on the Pt(111) surface at 600 K. The "thick" Ni layers were generated by exposing the Pt(111) substrate to Ni until the Pt(237 eV) Auger signal was within the noise level of the Auger spectra. A 95% signal attenuation requires about 8 ML of Ni coverage, assuming an IMFP for Pt(237 eV) electrons in Ni of 6.2 Å [11]. These "thick" Ni layers can be considered to be good model surfaces for Ni(111) single-crystal surfaces. They were characterized by a (1 × 1) fcc LEED pattern, and displayed surface reactivities similar to those reported in the literature for our probing molecules, as will be discussed below. In addition, they displayed LEED patterns similar to those reported for carbon on the Ni(111) single-crystal surface [15] after reaction with ethylene. We will abbreviate the description for these surfaces as Ni(111)/Pt(111) for the remainder of this article.

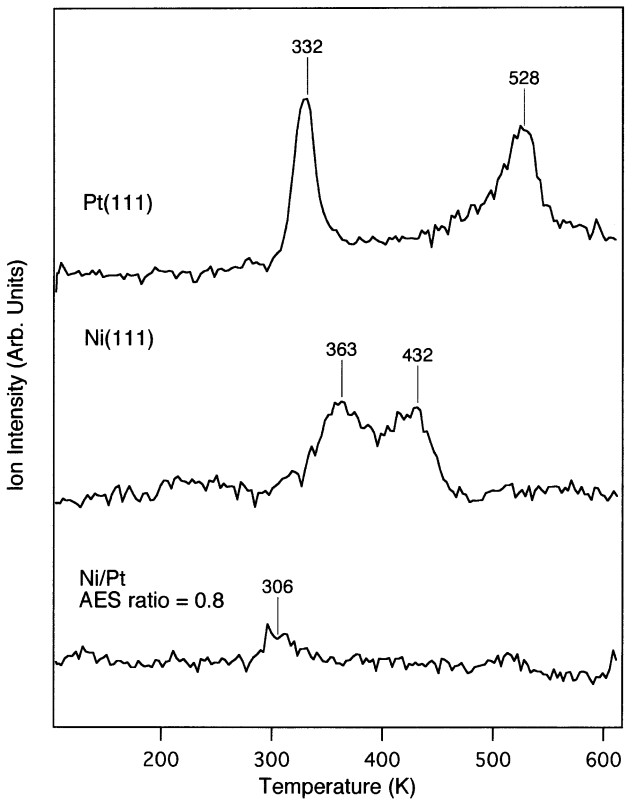


Figure 2. A comparison of TPD spectra of $H_2$ from the decomposition of 3 L ethylene on Pt(111), Ni(111)/Pt(111) and a Ni/Pt(111) bimetallic surface, $dT/dt = 3$ K/s.

### 3.2. Surface reactivities

In the following subsections, the surface reactivities of three different surfaces are compared by using ethylene and cyclohexene as probing molecules. These surfaces are clean Pt(111), "thick" Ni(111)/Pt(111), and Ni/Pt(111) bimetallic surfaces with a Ni(LMM)/Pt(237 eV) Auger peak-to-peak intensity ratio of ~ 1.0. Reactivities of the bimetallic surface were found to be distinctly different from either clean Pt(111) or Ni(111)/Pt(111) surface reactivities. These distinct reactivities, however, were most obvious at Ni(LMM)/Pt(237 eV) Auger peak-to-peak intensity ratios of ~ 1.0. If the Ni coverage deviated by as little as ~ 50% from this value, the observed surface reactivities began to resemble those of clean Pt(111) (for Ni coverages < 1 ML) or clean Ni(111)/Pt(111) (for Ni coverages > 1 ML). Therefore, only data from surfaces with a Ni(LMM)/Pt(237 eV) Auger peak-to-peak intensity ratio of ~ 1.0 will be presented here. For the remainder of this article, the description for these surfaces will be abbreviated with Ni/Pt(111)(AES $x$), where $x$ is the Ni(LMM)/Pt(237 eV) Auger peak-to-peak intensity ratio.

#### 3.2.1. Ethylene as probing molecule

Figure 2 shows a comparison of TPD spectra of $H_2$ from the decomposition of ethylene on Pt(111), Ni(111)/Pt(111), and a Ni/Pt(111) bimetallic surface (AES Ni/Pt = 0.8). Other than the parent molecule ethylene, $H_2$ was the only desorption species from all surfaces. The $H_2$ peak areas reach a saturation value at an exposure of 3 L for all three surfaces. Similar to previous studies [16], $H_2$ desorption from Pt(111) shows two desorption peaks, resulting from the formation of ethylidyne at ~ 332 K, and the further decomposition of this species beginning at ~ 528 K. On the Ni(111)/Pt(111) surface, $H_2$ desorption also leads to a two-peak spectrum at temperatures of ~ 363 and ~ 432 K. Our HREELS results suggest (see below) that the lower temperature desorption feature can be related to a desorption-limited $H_2$ recombination, with the surface hydrogen atoms being produced by the reaction of ethylene with the Ni(111)/Pt(111) surface to produce acetylene at lower temperatures. The higher temperature $H_2$ desorption peak can be attributed to a reaction-limited $H_2$ desorption, due to further decomposition of acetylene surface species. Despite the fact that both Ni(111)/Pt(111) and Pt(111) are highly reactive towards the decomposition of ethylene, the bimetallic Ni/Pt(111)(AES 0.8) surface displayed surprisingly little reactivity towards the probing molecule, as evidenced by the near absence of any $H_2$ desorption in figure 2. The peak area of the weak $H_2$ peak at 306 K is less than 10% of that of either Pt(111) or Ni(111)/Pt(111). This lack of

surface reactivity is also supported by the facts that we did not detect any other desorbing hydrocarbon molecules, such as ethane, acetylene or methane, in the TPD measurements. Furthermore, the inert nature of the Ni/Pt(111)(AES 0.8) surface is confirmed by AES measurements after the TPD experiments. For example, on Pt(111) and Ni(111)/Pt(111), the AES ratios of C(272 eV)/Pt(237 eV) and C(272 eV)/Ni(848 eV), after the TPD measurements, are 0.27 and 0.45, respectively. However, only negligible C(KLL) intensities were observed in AES after the TPD on the Ni/Pt(111) bimetallic surface.

HREELS spectra, following the surface reaction of ethylene with the Pt(111) and Ni(111)/Pt(111) surfaces, are shown in figures 3a and 3b, respectively. Both surfaces were exposed to 3 L of ethylene at 80 K, and then heated to the indicated temperatures for 30 s before spectral acquisition. All spectra were acquired after cooling to 80 K. The results in figure 3 are very similar to those reported previously for the surface reaction of ethylene with Pt(111) and Ni(111) [16,17], and will only be summarized briefly.

On Pt(111) (figure 3a), ethylene adsorbs in a di-$\sigma$-bonded fashion at 80 K [16]. The HREELS spectrum is characterized by the following vibrational features: $\nu_s$-Pt–C (460 $cm^{-1}$), $\rho$-$CH_2$ (778 $cm^{-1}$), $\tau_s$-$CH_2$ (994 $cm^{-1}$), $\nu$-CC (1042 $cm^{-1}$), $\omega_s$-$CH_2$ (1204 $cm^{-1}$), $\delta$-$CH_2$ (1430 $cm^{-1}$), $\nu_s$-$CH_2$ (2916 $cm^{-1}$) and $\nu_{as}$-$CH_2$ (2962 $cm^{-1}$) [16]. The di-$\sigma$-bonded geometry is retained on Pt(111) at 200 K, as evidenced by very little spectral change upon heating to this temperature. Upon heating to 300–450 K, an ethylidyne ($CCH_3$) intermediate is formed. The dominant vibrational features are observed at 419, 1116, 1339, and 2949 $cm^{-1}$, which are due to $\nu_s$-Pt–C, $\nu$-CC, $\delta_s$-$CH_3$ and $\nu_s$-$CH_3$ modes, respectively [16]. At $\sim$ 528 K, the ethylidyne species further decomposes into surface carbon and hydrogen (HREELS spectrum not shown), the latter recombines to desorb as $H_2$ as shown in the TPD spectrum in figure 2.

On Ni(111)/Pt(111) (figure 3b), ethylene is also strongly adsorbed in a di-$\sigma$ configuration at 80 K [17]. The corresponding HREELS spectrum at 80 K shows the following relatively intense features: $\nu_s$-Pt–C (446 $cm^{-1}$), $\nu_{as}$-Pt–C (662 $cm^{-1}$), $\rho$-$CH_2$ (873 $cm^{-1}$), $\nu$-CC (961 $cm^{-1}$), $\omega_s$-$CH_2$ (1103 $cm^{-1}$), $\delta$-$CH_2$ (1441 $cm^{-1}$) and $\nu_s$-$CH_2$ + $\nu_{as}$-$CH_2$ (2949 $cm^{-1}$) [17]. Upon heating to 200 K, the HREELS spectrum shows the formation of acetylene. This surface intermediate shows vibrational features at 446, 879, 1109, 1211 and 2915 $cm^{-1}$, which are due to $\nu$-Ni–C, $\rho_{as}$-CH, $\delta_s$-CH, $\nu$-CC, $\delta_{as}$-CH and $\nu$-CH vibrations of acetylene, respectively [17c]. After heating to 450 K, complete decomposition of the acetylene intermediate has occurred. Only the $\nu$-Ni–C mode remains in the spectrum. The HREELS results support our earlier suggestion that the lower temperature $H_2$ TPD feature in figure 2 is caused by desorption-limited

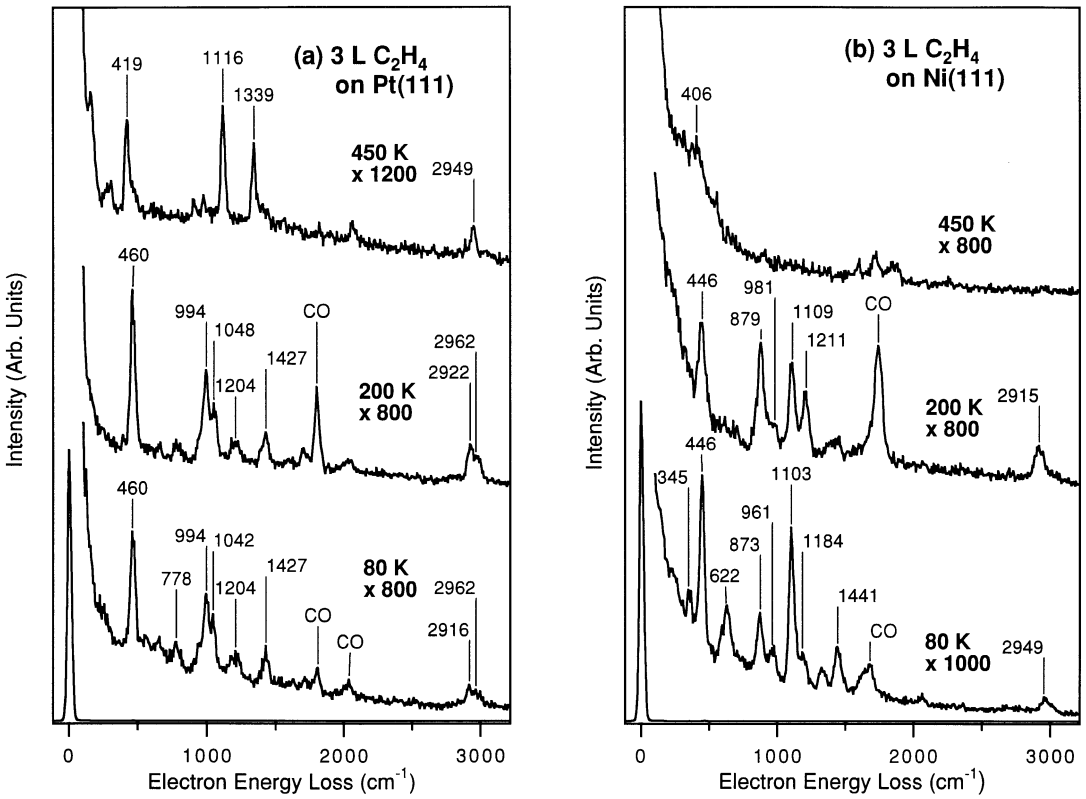


Figure 3. HREELS data following the reaction of ethylene on Pt(111) (a) and on Ni(111)/Pt(111) (b).

recombination of surface hydrogen. This argument is in agreement with the HREELS observation that acetylene (thus surface hydrogen) is produced on Ni(111)/Pt(111) at temperatures as low as 200 K. Recombinative $H_2$ desorption at approximate 363 K is consistent with the TPD results of atomic hydrogen on Ni(111)/Pt(111), as will be shown in figure 6. Furthermore, the combined HREELS and TPD results suggest that the higher temperature ($\sim$ 432 K) $H_2$ desorption peak from the Ni(111)/Pt(111) surface is a reaction-limited process and is due to the further decomposition of acetylene species. Figure 4 shows the HREELS spectra from the Ni/Pt(111)(AES 1.2) bimetallic surface after exposure to 3 L ethylene at 80 K, and after heating to 200 and 300 K. As suggested by the TPD results in figure 2, the interaction of the probing molecule with this bimetallic surface is substantially weaker than that with either clean Pt(111) or Ni(111)/Pt(111). The adsorbed molecule at 80 K is characterized by vibrational features at 419, 636, 920, 1062, 1218, 1434 and 2922 $cm^{-1}$. We tentatively assign these features to the $\nu_s$-M–C, $\nu_{as}$-M–C, $\omega_s$-$CH_2$, $\tau_s$-$CH_2$, $\nu$-CC, $\delta$-$CH_2$ and $\nu_s$-$CH_2$ vibrational modes, respectively. The weaker interaction of ethylene with the bimetallic surface is most clearly indicated by the strong enhancement in the relative intensity of the $\omega_s$-$CH_2$ mode at $\sim$ 920 $cm^{-1}$. For gas phase ethylene, the $\omega_s$-$CH_2$ mode is the only mode with a transition dipole moment perpendicular to the plane of the molecule. Its intensity relative to the other normal mode of the molecule is a sensitive measure of the degree of symmetry reduction as a result of a strong interaction with the surface upon adsorption [18]. As a result, the observation of a relatively intense $\omega_s$-$CH_2$ mode is generally associated with a weaker interaction between ethylene and the metal substrates [18]. The HREELS spectra in figure 4 were not significantly altered after heating to 200 K, suggesting no change in the bonding configuration of ethylene on the Ni/Pt(111)(AES 1.2) bimetallic surface. Upon heating to temperatures as low as 300 K, all hydrocarbon related vibrational features disappeared from the spectrum, indicating a weak and reversible interaction of ethylene with Ni/Pt(111). A significant amount of CO is also accumulated onto the free Ni/Pt(111) surface during the data acquisition. The lack of ethylene thermal decomposition from the HREELS (figure 4) and TPD (figure 2) data clearly demonstrates the reactivity of the Ni/Pt bimetallic surface is qualitatively different from that of either Pt(111) or Ni(111)/Pt(111).

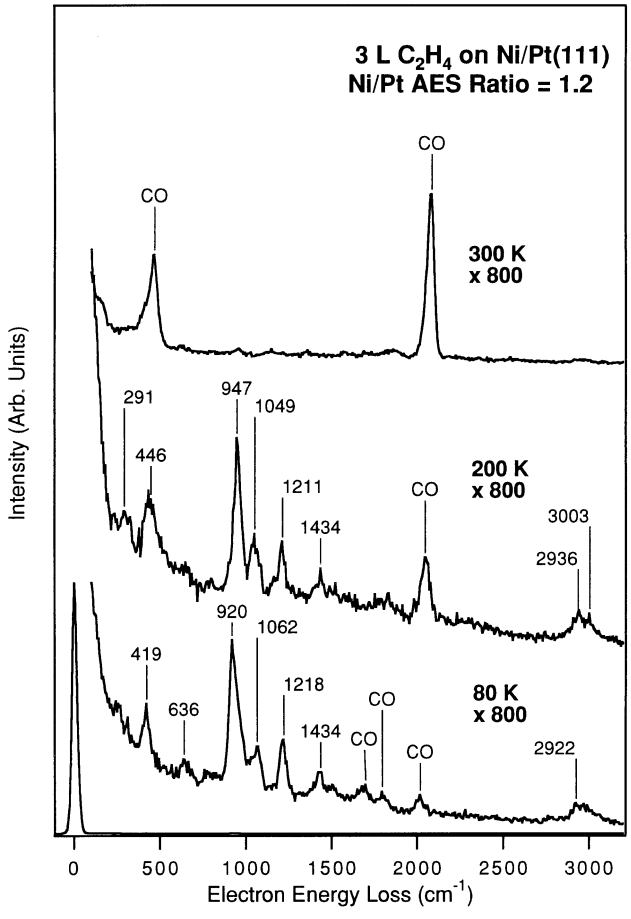


Figure 4. HREELS data following the reaction of ethylene on a Ni/Pt(111) bimetallic surface. The two intense features in the 300 K spectrum, at 440 and 2070 $cm^{-1}$, are related to the $\nu$-M–C and $\nu$-C–O modes, respectively, of residue CO molecules accumulated during data acquisition.

*3.2.2. Cyclohexene as probing molecule*

In this subsection we will show that, despite the lack of surface reactivity towards ethylene, the bimetallic Ni/Pt(111)(AES $\sim$ 1.0) surface does exhibit reactivity towards cyclohexene. However, the reaction pathway of cyclohexene on Ni/Pt(111) is unique when compared to either clean metal surface. Figure 5 shows results from TPD experiments after exposing the three different surfaces to 3 L of cyclohexene at 80 K. The 3 L exposure at 80 K resulted in coverages near one monolayer on Pt(111) [21]. Other than the molecular desorption, the only desorption products from the reaction of cyclohexene with the three types of surfaces were $H_2$, benzene and cyclohexane. All three surfaces are reactive towards cyclohexene as clearly evidenced by the desorption of $H_2$ as reaction products.

On clean Pt(111), the decomposition products from cyclohexene are $H_2$ and benzene. The desorption of $H_2$ desorption occurs mainly at temperatures of $\sim$ 302 and $\sim$ 409 K, with some weaker desorption peaks occurring at higher temperatures. Benzene desorption leads to an asymmetric peak at $\sim$ 404 K. The interaction of cyclohexene with this surface has been studied in great detail by Henn et al. [19] and by Pettiette-Hall et al. [20]. On the basis of these studies, the feature at 302 K can be related to a desorption-limited $H_2$ desorption (see also figure 6). The atomic hydrogen is produced by the formation of an allyl c-$C_6H_9$ species from cyclohexene in the temperature range of 200–240 K [19]. The higher temperature $H_2$

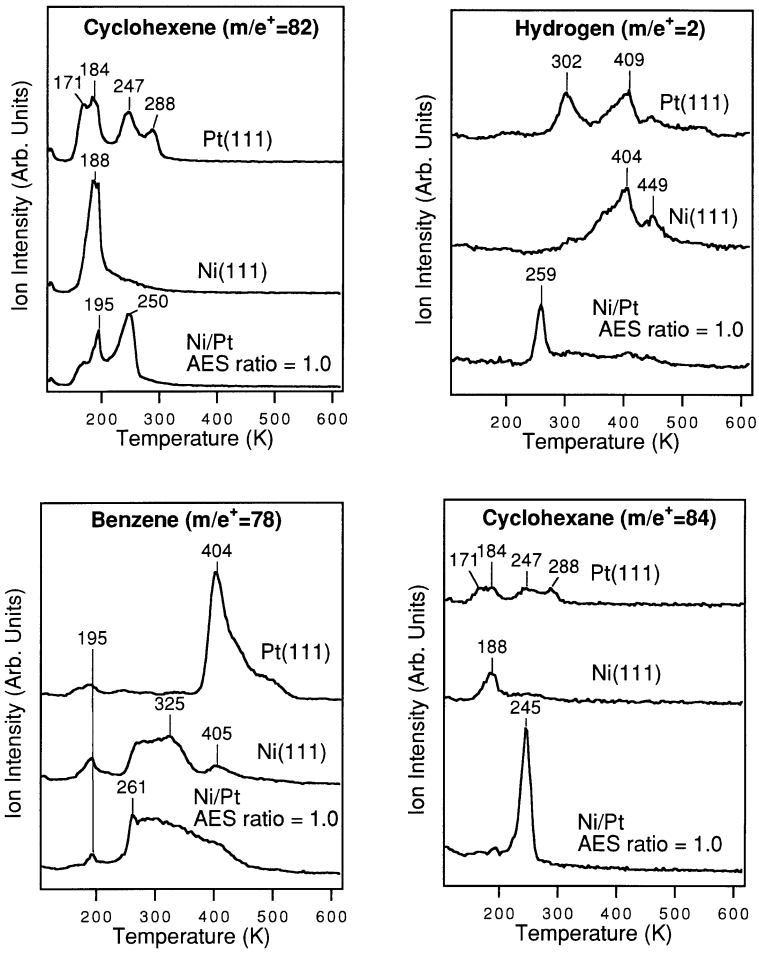


Figure 5. A comparison of TPD spectra of reaction products, $H_2$, benzene and cyclohexane, from the reaction of 3 L cyclohexene on Pt(111), Ni(111)/Pt(111) and a Ni/Pt(111) bimetallic surface.

TPD features are due to reaction-limited desorptions from the dehydrogenation of the allyl c-$C_6H_9$ intermediate to form benzene, and from the subsequent decomposition of benzene. Benzene decomposition competes with benzene desorption which produces a TPD feature at $\sim$ 404 K. The relative amounts of decomposition and desorption are strongly dependent on surface coverages [19–21].

The surface chemistry of cyclohexene on Ni(111) surfaces has not been as thoroughly studied. Similar as on the Pt(111) surface, the TPD results in figure 5 indicate that $H_2$ and benzene are the primary desorption products from the Ni(111)/Pt(111) surfaces. The desorption of $H_2$ occurred at $\sim$ 404 and $\sim$ 449 K, and benzene desorption resulted in a broad feature between 270 and 325 K and a smaller feature at 405 K. We will not attempt to give a detailed interpretation of the reaction mechanisms simply on the basis of TPD results. The main purpose of figure 5 is to demonstrate that hydrogen and benzene are the main decomposition products from cyclohexene on Ni(111)/Pt(111). More details on the combined HREELS and TPD studies of cyclohexene on Ni(111)/Pt(111), and on Ni/Pt(111) surfaces with various Ni coverages, will be discussed in a separate paper [22].

As on the Pt(111) and Ni(111)/Pt(111) surfaces, the reaction of cyclohexene with the bimetallic Ni/Pt(111)(AES 1.0) surface also led to the desorption of $H_2$ and benzene. However, unlike for either the Pt(111) or Ni(111)/Pt(111) surface, we also detected a relatively intense cyclohexane desorption feature at 245 K. In addition, on the bimetallic surface, $H_2$ desorption from reaction of cyclohexene occurred at a substantially lower temperature, as compared to either clean metal surface, as a sharp feature at 259 K. Benzene desorption resulted in a broad TPD feature between 260 and 450 K. It is also important to point out that the residue carbon concentrations following the reaction of cyclohexene, as estimated from AES measurements, are different for the three types of surfaces. On Pt(111) and Ni(111)/Pt(111), the AES ratios of C(272 eV)/Pt(237 eV) and C(272 eV)/Ni(848 eV), after the TPD measurements, are 0.23 and 0.48, respectively. However, only negligible C(KLL) intensities were observed in AES after the TPD of cyclohexene on the Ni/Pt(111) bimetallic surface.

The formation of cyclohexane from cyclohexene indi-

cates a substantially altered surface reactivity of the Ni/Pt(111)(AES 1.0) surface as compared to either pure metal surface. HREELS data, which will be published elsewhere [22], provides evidence that cyclohexene dehydrogenation to benzene on this bimetallic surface occurs at substantially lower temperature (< 200 K) than on either Pt(111) or Ni(111)/Pt(111) surface. The by-product of benzene, surface hydrogen, might react with cyclohexene to form cyclohexane on the Ni/Pt(111) bimetallic surface.

It is tempting to speculate that the metal–hydrogen bond strength and the related mobility of hydrogen on a given surface has a crucial impact on the resulting reaction pathways, especially on the rates of dehydrogenation and hydrogenation reactions. On the Ni/Pt(111)(AES 1.0) bimetallic surface the metal–hydrogen bond strength is substantially weaker than that of either pure metal surface. This can be inferred from TPD results shown in figure 6. Displayed in figure 6 are $D_2$ desorption spectra after exposing the clean Pt(111), clean Ni(111)/Pt(111) and Ni/Pt(111)(AES 1.0) surface to saturation exposures of hydrogen at 80 K. Recombinative $D_2$ desorption occurs at the lowest temperature (220 K) for the bimetallic surface and at temperatures of ~ 294 and ~ 379 K for the Pt(111) and Ni(111)/Pt(111) surfaces, respectively. It is of interest to note that experimental studies on the 50%Pt–50%Ni bulk alloys [23], as well as theoretical studies of Pt monolayers on Ni(111) [24], also showed a reduced chemisorption strength for atomic hydrogen as compared to either pure metal.

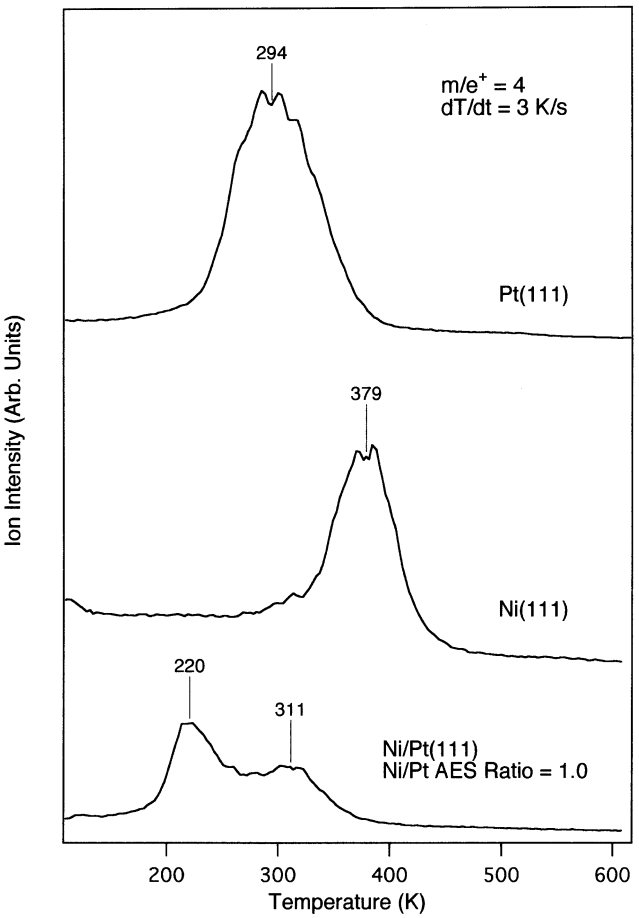


Figure 6. A comparison of TPD spectra of $D_2$ after a saturation exposure of 50 L $D_2$ on Pt(111), Ni(111)/Pt(111) and a Ni/Pt(111) bimetallic surface.

### 3.3. Structural and electronic modifications

One of the most important questions concerning the unique properties of bimetallic systems is whether the reactivities are modified by structural (ensemble) or electronic effects. For example, the lack of surface reactivity, for reactions requiring specific ensembles of surface atoms, is often explained in terms of site-blocking by adatoms [1,7], namely the structural modification effects. On the other hand, the electronic effects are related to the modification of electronic band structures due to the formation of metal–metal bonds, as demonstrated by Nørskov and coworkers in their calculations of the density of states (DOS) of several bimetallic systems [25].

In the current study, the use of ethylene as a probing molecule is an attempt to differentiate the structural and electronic modification effects on the reactivities of Ni/Pt(111). The reaction of ethylene with Pt(111) is characterized by the formation of di-$\sigma$-bonded ethylene species at 80 K followed by the formation of ethylidyne at $\geqslant$300 K. It is generally believed that the formation of ethylidyne on clean Pt(111) requires the presence of the three-fold sites on the fcc(111) oriented surface [16]. In addition, the formation of di-$\sigma$-bonded ethylene species and the subsequent production of acetylene on Ni(111)/Pt(111) should also require an ensemble of surface Ni atoms. However, in the case of the bimetallic Ni/Pt(111)(AES ~ 1.0) surface, neither ethylidyne nor acetylene is detected as reaction intermediate, despite the LEED observation that the Ni/Pt(111) surface retains its fcc(111) three-fold symmetry. In fact, the HREELS spectra in figure 4 indicate that the strongly bonded di-$\sigma$ ethylene species, which are required for the subsequent decomposition of ethylene, are never produced on the Ni/Pt(111) surface. Based on these observations, one could argue that the unique reactivity of Ni/Pt(111) is likely related to the lack of large assembles of either Pt or Ni surface atoms. However, more structural sensitive tools, such as tensor LEED [26], would be required to confirm the atomic-scale structure of the Ni/Pt(111) surfaces.

In conclusion, although the results presented here clearly demonstrate that the reactivity of the Ni/Pt(111) surface is qualitatively different from that of either Pt(111) or Ni(111)/Pt(111), they do not allow us to conclusively differentiate the structural and electronic modifications. However, we believe that the Ni/Pt(111)

surfaces can be used as good model systems for the understanding of the underlying factors that are generating the unique chemical properties in bimetallic systems. Detailed studies on the electronic properties of Ni/Pt(111) surfaces, using XPS for measuring the DOS of core level and valence band structures and near-edge X-ray absorption fine structure (NEXAFS) for probing the DOS of unoccupied d-band, are currently underway. In addition, band structure calculations, such as those performed by Nørskov and coworkers for several bimetallic systems [25], would also provide very important information on how the electronic properties are modified upon the formation of Ni–Pt bonds.

## 4. Conclusions

We have compared the surface reactivity of Ni/Pt(111) bimetallic surfaces with that of either pure metal surfaces by using ethylene and cyclohexene molecules as chemical probes. Ni/Pt(111) bimetallic surfaces characterized by a Ni(LMM)/Pt(237 eV) AES ratio near 1.0 displayed a unique surface reactivity, which was distinctly different from that of either clean Pt(111) or Ni(111)/Pt(111) surfaces. Both clean metal surfaces are highly reactive towards ethylene decomposition. On Pt(111) ethylene decomposes via the well documented ethylidyne intermediate, whereas on Ni(111)/Pt(111) the reaction proceeds via an acetylene intermediate. Quite surprisingly, the bimetallic surface showed very little reactivity towards ethylene despite the high reactivity of the pure metal components. In the reaction with cyclohexene all three surfaces displayed reactivity. The surface chemistry of the bimetallic Ni/Pt(111) surface, however, was unique in the formation of cyclohexane from cyclohexene, which is not observed on either pure metal surface. We believe that the Ni/Pt(111) surface provides a good model system for future studies of the differentiation of electronic and structural modifications that are controlling the unique reactivity of bimetallic systems.

## References

[1] J.H. Sinfelt, Acc. Chem. Res. 10 (1977) 15.
[2] W.M.H. Sachtler and R.A. van Santen, Adv. Catal. 26 (1977) 69.
[3] J.K.A. Clarke, Chem. Rev. 75 (1975) 291.
[4] V. Ponec, Adv. Catal. 32 (1983) 149.
[5] E. Bauer, in: *The Chemical Physics of Solid Surfaces and Heterogeneous Catalysis*, Vol. 3, eds. D.A. King and D.P. Woodruff (Elsevier, Amsterdam, 1984).
[6] C.T. Campbell, Ann. Rev. Phys. Chem. 41 (1990) 775.
[7] J.A. Rodriguez, Surf. Sci. Rep. 24 (1996) 223.
[8] B. Frühberger and J.G. Chen, Surf. Sci. 342 (1995) 38.
[9] M. Sambi, E. Pin and G. Granozzi, Surf. Sci. 340 (1995) 215.
[10] M.P. Seah, in: *Practical Surface Analysis*, 2nd Ed. (Wiley, New York, 1996) ch. 5.
[11] S. Tanuma, C.J. Powell and D.R. Penn, Surf. Interf. Anal. 11 (1988) 577.
[12] (a) C. Argile and G.E. Rhead, Surf. Sci. Rep. 10 (1989) 277;
(b) A.J. Slavin, Prog. Surf. Sci. 50 (1995)159;
(c) W.F. Egelhoff Jr., in: *Ultrathin Magnetic Structures I*, An Introduction to Electronic, Magnetic and Structural Properties (Springer, Berlin, 1994).
[13] (a) M. Galeotti, A. Atrei, U. Bardi, B. Cortigiani, G. Rovida and M. Torrini, Surf. Sci. 297 (1993) 202, and references therein;
(b) N.T. Barrett, R. Belkhou, J. Thiele and C. Guillot, Surf. Sci. 331–333 (1995) 776.
[14] P.M. Holmblad, J. Hvolbæk Larsen, I. Chorkendorff, L. Pleth Nielsen, F. Besenbacher, I. Stensgaard, E. Lægsgaard, P. Kratzer, B. Hammer and J.K. Nørskov, Catal. Lett. 40 (1996) 131.
[15] A. Grossmann, W. Erley and H. Ibach, Surf. Sci. 337 (1995) 183.
[16] H. Steininger, H. Ibach and S. Lehwald, Surf. Sci. 117 (1982) 685.
[17] (a) J.E. Demuth, Surf. Sci. 76 (1978) L603;
(b) J.E. Demuth, H. Ibach and S. Lehwald, Phys. Rev. Lett. 40 (1978) 1044;
(c) S. Lehwald and H. Ibach, Surf. Sci. 89 (1979) 425;
(d) X.-Y. Zhu and J.M. White, Surf. Sci. 214 (1989) 240;
(e) X.-Y. Zhu, M.E. Castro, S. Akhter and J.M. White, J. Vac. Sci. Technol. A 7 (1989) 1991.
[18] (a) H. Ibach and D.L. Mills, *Electron Energy Loss Spectroscopy and Surface Vibrations* (Academic Press, New York, 1982);
(b) N. Sheppard, Ann. Rev. Phys. Chem. 39 (1989) 589, and references therein;
(c) B. Frühberger and J.G. Chen, J. Am. Chem. Soc. 118 (1996) 11599.
[19] F.C. Henn, A.L. Diaz, M.E. Bussell, M.B. Hugenschmidt, M.E. Domagala and C.T. Campbell, J. Phys. Chem. 96 (1992) 5965.
[20] C.L. Pettiette-Hall, D.P. Land, R.T. McIver Jr. and J.C. Hemminger, J. Am. Chem. Soc. 113 (1991) 2755.
[21] J.G. Chen and B. Frühberger, Surf. Sci. Lett. 367 (1996) L102.
[22] J.G. Chen and B. Frühberger, in preparation.
[23] J. Massardier, B. Tardy, P. Delichère, M. Abon and J.C. Bertolini, *Proc. 8th Int. Congr. on Catalysis*, Vol. IV (Verlag Chemie, Weinheim, 1984) p. 185.
[24] N.J. Castellani, P. Légaré, C. Demangeat and S. Pick, Surf. Sci. 352–354 (1996) 148.
[25] B. Hammer and J.K. Nørskov, Surf. Sci. 366 (1996) 394.
[26] D. Jentz, S. Rizzi, A. Barbieri, D.G. Kelly, M.A. Van Hove and G.A. Somorjai, Surf. Sci. 329 (1995) 14.